Published in final edited form as:

PET Clin. 2018 October ; 13(4): 623–634. doi:10.1016/j.cpet.2018.05.012.

Applications of PET/CT and PET/MR Imaging in Primary Bone Malignancies

Ashkan Heshmatzadeh Behzadi, MD[a,*], **Syed Imran Raza, MBBS**[a], **John A. Carrino, MD, MPH**[b], **Christos Kosmas, MD**[c], **Ali Gholamrezanezhad, MD**[d], **Kyle Basques, MD**[c], **George R. Matcuk Jr, MD**[d], **Jay Patel, MD**[a], **Hossein Jadvar, MD, PhD, MPH, MBA**[e]

[a]Department of Radiology, Weill Cornell Medical Center, 525 East 68th Street, New York, NY 10065, USA;

[b]Department of Radiology and Imaging, 535 East 70th Street, Hospital for Special Surgery, New York, NY 10021, USA;

[c]Department of Radiology and Imaging, University Hospitals of Cleveland, Case Western Reserve University, 10900 Euclid Avenue, Cleveland, OH 44106, USA;

[d]Division of Musculoskeletal Radiology, Department of Radiology, Keck School of Medicine, University of Southern California (USC), Los Angeles, CA 90007, USA;

[e]Division of Nuclear Medicine, Department of Radiology, Keck School of Medicine, University of Southern California, Los Angeles, CA 90007, USA

Keywords

PET/CT; PET/MRI; Primary bone malignancies

INTRODUCTION

Diagnostic imaging plays a central role in the evaluation and management of oncologic disease involving the musculoskeletal system (Figs. 1–5). Standard imaging modalities used in current practice include conventional radiography, computed tomography (CT) scanning, Magnetic resonance imaging (MRI), and skeletal scintigraphy.[1,2] In recent years, PET imaging has also emerged as a complementary modality in musculoskeletal imaging, using various radiopharmaceutical agents to improve detection and characterization of the pathophysiology of disease.[3] Fusion of PET-acquired images with CT scans or MRI has significantly improved the overall diagnostic accuracy.[4] The objective of this article is to review the current role of PET/CT scans and PET/MRI hybrid imaging in the evaluation of primary malignancies of the skeletal system, with an emphasis on clinical usefulness, imaging findings, and current limitations.

[*]Corresponding author. Department of Radiology, Weill Cornell Medical College, 416 East 55th Street, New York, NY 10022. ashkan.hbehzadi@gmail.com.

ROLE OF HYBRID IMAGING IN BONE MALIGNANCY

Viable malignant primary bone tumors are usually 18F-fluorodeoxyglucose (FDG) avid.[4,5] PET imaging using FDG produces images that allow for the diagnosis of these neoplasms, initial staging, selection of biopsy sites, evaluation of treatment response, and assessment for tumor recurrence.[3,4,6,7] When CT images are contemporaneously acquired, the PET and CT data are spatially co-registered, allowing for significantly improved localization of metabolic abnormalities. Integrated PET/CT devices allow for reduced scanning time and improved PET image quality and quantitation using CT attenuation correction reconstruction techniques.[6]

In the FDG PET component of these studies, lesions are assessed primarily based on their maximum standardized uptake value (SUV_{max}) and graded accordingly.[8] As methods evolve, metabolic activity will become a useful marker for differentiating between benign and malignant lesions. Moreover, dual time point imaging, which involves measuring the SUV_{max} at multiple sequential intervals after radiotracer injection, may also be beneficial in differentiating benign lesions from malignant processes.[9–11]

Recently, interest in hybrid PET/MRI has grown, particularly in evaluation of the musculoskeletal system. This new modality couples the physiologic information acquired from PET with the unparalleled soft tissue resolution and contrast of MRI to provide more accurate diagnoses.[12] In addition, MRI can be used to provide additional functional information using perfusion techniques and diffusion-weighted imaging.[13–15] With hybrid PET/MRI, a patient's oncologic disease can potentially be fully characterized and staged in a single imaging session.[14]

The morphologic characteristics of tumors are critical in making the correct diagnosis.[2,7,16] The MRI and CT components of hybrid imaging provide important morphologic information that PET scans alone cannot provide and, therefore, it is essential that the interpreting radiologist be familiar with the conventional imaging appearance of bone tumors.[9,10] The morphologic characteristics of lesions can be preliminarily evaluated on the whole-body CT or MRI portion of the examination, which is obtained contemporaneously with the PET dataset, and then further correlated with dedicated small field-of-view MRI sequences or other anatomic imaging as necessary.[2,4,17]

CLINICAL APPLICATIONS

Osteosarcoma

Osteosarcoma is the most common primary malignant bone tumor.[18,19] Accurate initial staging and restaging after treatment is critical to patient care. Prognosis strongly depends on tumor size and the presence of metastatic disease at initial presentation. To put this into perspective, the 5-year survival decreases drastically from 70.1% in localized disease to 31.6% in the presence of metastasis.[20–24] Response to preoperative neoadjuvant chemotherapy is also a very important prognostic factor for disease-free survival.[25,26]

Imaging plays a key role in the management of osteosarcoma, with the initial diagnosis frequently made with conventional radiography, and with local staging performed with MRI to assess local soft tissue extension, bone marrow infiltration, and the presence of osseous skip lesions.[20,21] FDG PET scanning has a promising role in the management of osteosarcoma given its ability to help distinguish viable primary and recurrent neoplasm from successfully treated disease and benign entities.

Like most other malignant tumors, osteosarcoma has an increased rate of glycolysis and consequently demonstrates increased uptake of FDG.[4] Therefore, FDG PET readily demonstrates local and systemic sites of activity that correlate well with disease severity.[27,28] FDG PET/CT scanning is highly useful for the evaluation of osteosarcoma, with a sensitivity of nearly 100% in initial staging, 85.7% in locally recurrent disease, and 95% in identifying distant metastasis.[29,30] Although PET/CT scanning has some limitations in the evaluation of pulmonary and lymph node metastases, it has been shown to have superior accuracy over bone scans in the detection of osseous dissemination.[29,30]

One of the main strengths of FDG PET scanning in osteosarcoma is in determining the metabolic response to treatment. SUV measurements have been found to parallel histopathologic findings, with high SUV values correlating with increased mitotic counts and lower values corresponding with areas of tumor necrosis. For example, Cheon and colleagues[25] and Ye and colleagues[26] demonstrated that a reduction in SUV_{max} after chemotherapy correlates well with degree of tumor necrosis and subsequent patient outcome. In a recent study, Davis and colleagues[27] followed 34 patients with osteosarcoma and surveyed SUV_{max} on routine posttreatment surveillance for up to 10 weeks. The percent change of SUV_{max} from baseline to week 10 served as a metabolic predictor that correlated well with histologic response to therapy. A separate metaanalysis of 8 studies comprising 178 patients with osteosarcoma found that a postchemotherapy SUV_{max} of 2.5 or less and a ratio of SUV_{max} posttherapy to SUV_{max} pretherapy of 0.5 or less was a valuable predictor of histologic response to chemotherapy.[31] In another prospective study assessing therapeutic response in pediatric osteosarcomas, FDG PET scanning was also able to help discriminate responders from nonresponders.[31] Hence, PET/CT scanning may play an important role in the early identification of patients who are not responding to treatment and may benefit from a change in therapy.

FDG PET scanning also holds promise in its ability to distinguish posttherapy changes from disease recurrence, a challenging but important task. Studies have shown that FDG-PET can differentiate posttreatment changes from disease recurrence with greater sensitivity and specificity than other imaging modalities.[32] In particular, the degree of FDG uptake as calculated by SUV_{max} may be helpful in distinguishing viable osteosarcoma from treated disease.[24] Although there remain some overlap in ranges of SUV values between malignant and nonmalignant processes, work continues to refine measurement techniques and guidelines to improve the specificity of FDG PET scanning.[28,33]

Although the value of PET/MRI for the staging and follow-up of osteosarcoma has not yet been well-established, some promising early results have been observed.[34,35] A study by Eiber and colleagues[36] compared the performance of PET/MRI and PET/CT scanning for

the detection of bone lesions. These investigators found that anatomic localization and allocation of PET-positive lesions was superior on PET/MRI compared with PET/CT scanning, whereas detection and characterization was found to be on par with PET/CT scanning, possibly owing to inclusion of primarily FDG-avid lesions. The SUV_{mean} in bone lesions was on average 12.4% ± 15.5% lower for PET/MRI than for PET/CT scanning, although this difference between modalities was not statistically significant.

At present, MRI is the preferred imaging modality for local tumor staging of osteosarcoma. PET scanning lends itself well to nodal staging, whereas PET scanning and MRI together are highly accurate for the detection of metastases.[34] Hence, whole body PET/MRI with concurrent diagnostic MRI imaging of the primary site of osteosarcoma can allow for complete TNM staging in a single session, providing convenience and resource savings as well as decreasing radiation exposure. In addition, the PET component can guide diagnostic biopsies and in turn allow for correct staging and grading, with subsequent impact on treatment selection and outcome.[16,34]

Ewing's Sarcoma

Ewing's sarcoma is the second most common primary malignancy of bone, with a peak incidence in children and adolescents aged 4 to 15 years. FDG PET/CT scanning has become a valuable imaging modality in staging, restaging, and assessment of treatment response in patients with Ewing's sarcoma, largely owing to its ability to provide metabolic information that is, not feasible with other modalities.[37–39]

Similar to the case with osteosarcoma, MRI is mainstay imaging in staging of Ewing's sarcoma. However, both MRI and CT imaging are limited in distinguishing viable from nonviable neoplastic tissues.[38,40] FDG PET scanning has been shown to detect tumor progression and regression even before morphologic alterations are seen on conventional imaging modalities, based on differences in intensity of FDG uptake.[35,37,41] PET/CT scanning in particular is already in use for this purpose in Ewing's sarcoma, and is able to differentiate viable from nonviable tumor with high sensitivity and specificity.[42] Typical viable Ewing's sarcoma demonstrates SUVs ranging from 3 to 10, with higher values correlating well with higher tumor grade. PET/CT scanning is also highly efficacious in detecting lymph node and bone metastases, with sensitivity values of 90% to 98% compared with 25% to 83% for conventional imaging methods, with good specificity as well (97% for PET/CT scanning vs 78% for conventional imaging).[41,43] The exception was in the detection of lung metastases, which was more accurate with CT scanning.[41]

Besides providing prognostic data, findings on PET/CT scanning during and after treatment can also guide decision making about continuing or altering therapy in patients with Ewing's sarcoma. For example, a study by Bredella and colleagues[44] demonstrated that a 30% decrease or increase in SUV reliably distinguished between adequate response to therapy and progression of disease, respectively. In addition, Hawkins and colleagues[45] showed that patients with tumors displaying a SUV_{max} of less than 2.5 after neoadjuvant chemotherapy demonstrated an improvement in 4-year progression-free survival compared with those with higher SUV_{max} (72% vs 27%, respectively) and that this effect was independent of initial disease stage.

A major limitation of PET/CT scanning in the pediatric population predominantly affected by Ewing's sarcoma is the relatively high radiation dose, particularly compared with whole body MRI, which does not involve ionizing radiation.[39] The introduction of whole-body PET/MRI allows for simultaneous regional staging and whole body evaluation for metastatic disease.[6,12] PET/MRI is especially helpful in overcoming some of the limitations of PET/CT scanning, specifically in the evaluation of disease in organs with relatively high background activity such as the brain, liver, kidney, and spinal canal.[7,13,14] PET/MRI may soon become the imaging modality of choice for staging of Ewing's sarcoma.

Chondrosarcoma

The diagnosis of chondrosarcoma can be challenging owing to the diverse nature of chondral neoplasms, the significant overlap with benign entities on conventional imaging, and difficulties in accurate sampling on tissue biopsy owing to tumor heterogeneity. FDG PET scanning was initially dismissed as an unreliable modality in the evaluation of chondroid neoplasms, but recent literature has demonstrated promising results. Generally, benign chondroid lesions such as enchondromas and osteochondromas are not FDG avid (SUV_{max} < 2). In contrast, most chondrosarcomas demonstrate low-grade FDG avidity (SUV_{max} > 2), with variable metabolic activity seen ranging from SUV_{max} of 1.3 to 12.4. SUV_{max} has been shown to correlate with tumor grade.[46–49] Unfortunately, there is significant overlap in SUV_{max} values between benign and malignant chondroid lesions, with SUV_{max} values between 2.0 and 4.5 having particularly poor specificity, and with up to 46% of lesions reported in a recent metaanalysis having SUV_{max} values in this range. However, recent large studies have demonstrated that, overall, when using an SUV_{max} threshold of 2.2 to 2.3, the sensitivity and specificity exceeds 90% in differentiating between benign/low-grade lesions from high-grade chondroid neoplasms.[46–51] Classifying lesions between benign/low-grade lesions and high-grade neoplasms helps clinicians to decide whether observation or active treatment is the optimal treatment strategy.[47,48]

The heterogeneity of chondroid tumors poses an ever-present risk of undersampling during biopsy and difficulty in obtaining appropriate excisional margins. FDG PET scanning ameliorates this problem by providing direct visual and quantitative assessment of tumor metabolic activity and extent. By targeting regions for biopsy with the greatest metabolic activity, radiologists and surgeons can reduce core needle biopsy sampling error, and consequently, the rate of false-negative biopsies. Subsequent correlation of imaging findings with histopathology also helps eliminate the potential error of undersampling.[46,50,51] In addition, as in other sarcomas, whole body imaging in PET/CT scanning can be used for initial staging of chondrosarcoma and as an adjunct in postoperative imaging surveillance.[52]

There is a paucity of data on the use of PET/MRI in chondrosarcoma. One study by Purohit and colleagues[53] assessed laryngeal chondrosarcomas using PET/MRI, showing that PET/MRI successfully highlights regions of hypermetabolic dedifferentiated neoplasm (with concurrent low apparent diffusion coefficient values on diffusion-weighted imaging MRI sequences) in a background of hypo-metabolic, low-grade chondroid tissue. These investigators concluded that PET/MRI can provide additional functional information to supplement the morphologic mapping and histopathology of these tumors. Given the

importance of accurate characterization of these heterogeneous lesions, it is expected that future research will highlight a potential role for PET/MRI in the management of chondrosarcoma.

Primary Bone Lymphoma

Primary bone lymphoma is an extranodal lymphoma that arises from the medullary cavity and manifests as a localized solitary lesion. Primary bone lymphoma is relatively uncommon, representing only 1% of all malignant lymphomas.[54,55,56] The tumor favors sites of persistent bone marrow formation, such as the femur, pelvis, tibia, fibula, and humerus.[54,56,57]

The role of FDG PET/CT scanning in the diagnosis, staging, and restaging of Hodgkin disease and non-Hodgkin lymphoma is well-established.[58,59] Accurate staging is essential for treatment planning and provides important prognostic information. PET/CT scanning can detect lymphoma with 90% sensitivity and 91% specificity, although overall positive predictive value is low, especially for disease progression.[59]

The usual appearance of primary bone lymphoma on FDG PET scanning is as a focal hypermetabolic lesion. There are few reports on the initial diagnosis of primary bone lymphomas using FDG PET or PET/CT scanning.[56,60,61] However, studies have demonstrated PET/CT scanning to be an effective modality for evaluation after therapy, particularly in documenting treatment response. In patients who respond successfully to treatment, FDG PET scanning will show a rapid decline in FDG uptake compared with baseline imaging. Similarly, any newly identified FDG-avid lesions are deemed to be recurrences. Hence, PET/CT scanning has the potential to assist in the management of patients with primary bone lymphoma.[62,63]

PET/MRI has shown encouraging results in early studies.[64,65] Sensitivity for assessment of disease burden is similar in PET/MRI and PET/CT scanning. In addition, the added information from diagnostic MRI sequences can help to characterize changes in the cellular content of lesions, particularly using diffusion-weighted imaging sequences and MRI spectroscopy.[64,66]

Multiple Myeloma

Multiple myeloma (MM) is a debilitating malignancy that is part of a spectrum of diseases ranging from monoclonal gammopathy of unknown significance to plasma cell leukemia.[67] The use of conventional radiography has traditionally been used in cases of newly diagnosed or relapsed myeloma, with the whole body skeletal survey used to assess extent of disease.[68] Radiographs typically demonstrate focal osteolytic lesions, but have a lower sensitivity in diffuse osseous involvement. They also do not provide any indication of disease activity except by monitoring changes over time.

FDG PET/CT scanning has been shown to have high sensitivity, specificity, and prognostic value in patients with MM, superior to conventional radiographs and comparable with MRI, providing valuable prognostic and therapy assessment information for the management of patients.[69] In a systematic review consisting of almost 800 patients with MM, FDG PET/CT

scanning had a sensitivity and specificity of 80% to 90% and 80% to 100%, respectively, in the detection of osteolytic lesions.[70] Clinical use of FDG PET/CT scanning in myeloma has been validated in recent years with the revised Durie/Salmon PLUS staging system.[71] PET also has the advantage of identifying the degree of metabolic activity associated with focal lesions, which has been found to correlate with disease activity.[72,73] Solitary plasma cell neoplasms (plasmacytomas) are also FDG avid.[72,73] However, FDG PET scanning is somewhat less reliable when evaluating more diffuse or heterogeneous marrow involvement, with variable SUV measurements.[7] In addition, differentiating myelomatous lesions from background marrow FDG uptake can be difficult, particularly in the setting of diffuse marrow involvement.[7]

MRI in myeloma demonstrates T2 hyperintensity and T1 hypointensity in involved areas of bone, with variable contrast enhancement seen. The overall MRI pattern may be described as normal, focal, diffuse (change of signal of the entire fatty bone marrow), or a variegated/salt-and-pepper pattern (heterogeneous appearance of the entire bone marrow).[7]

Zamagni and colleagues[74] prospectively compared FDG PET/CT scanning, MRI, and whole body planar radiographs in the assessment of bone disease in 23 patients with newly diagnosed MM. PET/CT scanning was superior to plain radiographs, and highly sensitive to lesions out of the field of view of MRI, for both intramedullary and extramedullary disease. However, PET/CT scanning failed to depict some spine and pelvic lesions detected on MRI. A study by Shortt and colleagues[75] showed that a combination of data acquired from PET and whole body MRI improved specificity and positive predictive value. Bartel and colleagues[69] performed FDG PET/CT scanning in 239 patients at baseline and after neoadjuvant therapy, but before stem cell transplantation. Better overall and event-free survivals were correlated with complete normalization of FDG PET uptake before autologous stem cell transplantation.

Most studies and review articles pertaining to PET scanning and MRI have examined the 2 modalities separately.[76] However, preliminary reports suggest a role for combined PET/MRI in MM and other plasma cell dyscrasias. With the ability to image the whole body using both PET scanning and MRI, each of which can assess lesion distribution and characteristics, PET/MRI offers unique opportunities for assessing disease burden, monitoring for progression, and assessing response to treatment. For example, recent studies have demonstrated that PET/MRI can be effective in high-risk patients for initial staging and can serve as a baseline to assess treatment response as well as relapse of disease. If a patient's biochemical marker levels are increasing after therapy, PET/MRI can be used to assess for the presence of new lesions or an increase in size, avidity, or number of lesions on PET scanning.[7,76]

Giant Cell Tumor

Giant cell tumor of bone (GCT) is an uncommon primary intramedullary neoplasm, most prevalent in young adults. GCT is generally considered to be benign. However, these lesions are variable in behavior and can be locally aggressive, have a high local recurrence rate after treatment (up to 40%), and may even produce pulmonary metastases.[77,78] The management of GCT can be challenging and sometimes controversial.

On radiography and CT scanning, GCT typically manifests as an eccentric lytic lesion centered in the epiphysis of a long bone that extends to the articular surface and usually has a well-defined nonsclerotic margin. On MRI, GCT is hypointense on T1-weighted sequences, and heterogeneously intermediate to hypointense on T2-weighted sequences related to hemosiderin deposition within the tumor.[77]

On PET scanning, GCT tends to have an unusually high FDG uptake compared with other benign neoplasms of bone, and may be misdiagnosed as a malignant lesion.[51,78–81] A recent study by Muheremu and colleagues[82] demonstrated a mean lesional SUV_{max} of 9.2 ± 3.8 in 20 patients with proven GCT. Therefore, it is important to consider the diagnosis of GCT as well as soft tissue sarcomas in solitary musculoskeletal lesions with high FDG uptake.

Evaluation for pulmonary metastases of GCT can be challenging on PET. When lesions are small, they resemble pulmonary nodules, whose characterization is limited by their small size and limited spatial resolution of PET. In addition, over time these metastases can grow and show significant FDG uptake, mimicking primary malignant pulmonary lesions.[83] PET/CT scanning has been recognized as a valuable tool for early response evaluation of GCTs to new treatment options, such as denosumab.[84–87]

SUMMARY

The hybrid modalities of FDG PET/CT scanning and PET/MRI have transformed oncologic imaging by providing whole body scans that combine the sensitivity of metabolic imaging with the specificity of anatomic imaging. FDG PET/CT scanning has usefulness in the diagnosis, staging, and assessment of therapeutic response to treatment of several primary musculoskeletal malignancies. Although data on PET/MRI are limited at present, emerging studies demonstrate potentially promising applications, which allows for detailed local staging and tissue characterization, all while reducing patient's exposure to radiation.

REFERENCES

1. Hilner BE, Siegel BA, Liu D, et al. Impact of positron emission tomography/computed tomography and positron emission tomography (PET) alone on expected management of patients with cancer: initial results from the National Oncologic PET Registry. J Clin Oncol 2008;26:2155–61. [PubMed: 18362365]
2. Lakkaraju A, Patel CN, Bradley KM, et al. PET/CT in primary musculoskeletal tumours: a step forward. Eur Radiol 2010;20(12):2959–72. [PubMed: 20577880]
3. Blodgett TM, Meltzer CC, Townsend DW. PET/CT: form and function. Radiology 2008;242:360–85.
4. Choi YY, Kim JY, Yang SO. PET/CT in benign and malignant musculoskeletal tumors and tumor-like conditions [review]. Semin Musculoskelet Radiol 2014;18(2):133–48. [PubMed: 24715446]
5. Watabe T, Shimosegawa E, Kato H, et al. Paradoxical reduction of cerebral blood flow after acetazolamide loading: a hemodynamic and metabolic study with (15)O PET. Neurosci Bull 2014;30: 845–56. [PubMed: 25096497]
6. Disselhorst JA, Bezrukov I, Kolb A, et al. Principles of PET/MR imaging. J Nucl Med 2014;55:2S–10S. [PubMed: 24819419]
7. Chaudhry AA, Gul M, Gould E, et al. Utility of positron emission tomography-magnetic resonance imaging in musculoskeletal imaging [review]. World J Radiol 2016;8(3):268–74. [PubMed: 27027320]

8. Aoki J, Watanabe H, Shinozaki T, et al. FDG PET of primary benign and malignant bone tumors: standardized uptake value in 52 lesions. Radiology 2001;219:774–7. [PubMed: 11376267]
9. Tian R, Su M, Tian Y, et al. Dualtime point PET/CT with F-18 FDG for the differentiation of malignant and benign bone lesions. Skeletal Radiol 2009;38: 451–8. [PubMed: 19205695]
10. Zhuang H, Pourdehnad M, Lambright ES, et al. Dual time point 18FFDG PET imaging for differentiating malignant from inflammatory processes. J Nucl Med 2001;42:1412–7. [PubMed: 11535734]
11. Hogendoorn PC, Athanasou N, Bielack S, et al., ESMO/EUROBONET Working Group. Bone sarcomas: ESMO clinical practice guidelines for diagnosis, treatment and follow-up. Ann Oncol 2010;21(Suppl 5):v204–13. [PubMed: 20555083]
12. Werner MK, Schmidt H, Schwenzer NF. MR/PET: a new challenge in hybrid imaging. AJR Am J Roentgenol 2012;199:272–7. [PubMed: 22826387]
13. Partovi S, Kohan AA, Zipp L, et al. Hybrid PET/MR imaging in two sarcoma patients - clinical benefits and implications for future trials. Int J Clin Exp Med 2014;7:640–8. [PubMed: 24753758]
14. Fahey FH, Treves ST, Adelstein SJ. Minimizing and communicating radiation risk in pediatric nuclear medicine. J Nucl Med Technol 2012;40:13–24. [PubMed: 22393223]
15. Hirsch FW, Sattler B, Sorge I, et al. PET/MR in children. Initial clinical experience in paediatric oncology using an integrated PET/MR scanner. Pediatr Radiol 2013;43:860–75. [PubMed: 23306377]
16. Dehdashti F, Siegel BA, Griffeth LK, et al. Benign versus malignant intraosseous lesions: discrimination by means of PET with 2-[F-18] flouro-2- deoxy-D-glucose. Radiology 1996;200:243–7. [PubMed: 8657920]
17. Costelloe CM, Chuang HH, Madewell JE. FDG PET/CT of primary bone tumors [review]. AJR Am J Roentgenol 2014;202(6):W521–31. [PubMed: 24848845]
18. Strobel K, Exner UE, Stumpe KD, et al. The additional value of CT images interpretation in the differential diagnosis of benign vs. malignant primary bone lesions with 18F-FDGPET/CT. Eur J Nucl Med Mol Imaging 2008;35:2000–8. [PubMed: 18712385]
19. Marulanda GA, Henderson ER, Johnson DA, et al. Orthopedic surgery options for the treatment of primary osteosarcoma. Cancer Control 2008;15(1): 13–20. [PubMed: 18094657]
20. Vander Griend RA. Osteosarcoma and its variants. Orthop Clin North Am 1996;27(3):575–81. [PubMed: 8649738]
21. Franzius C, Sciuk J, Daldrup-Link HE, et al. FDG PET for detection of osseous metastases from malignant primary bone tumours: comparison with bone scintigraphy. Eur J Nucl Med 2000;27:1305–11. [PubMed: 11007511]
22. Daldrup-Link HE, Franzius C, Link TM, et al. Whole-body MR imaging for detection of bone metastases in children and young adults: comparison with skeletal scintigraphy and FDG PET. Am J Roentgenol 2001;177:229–36. [PubMed: 11418435]
23. Even-Sapir E, Metser U, Flusser G, et al. Assessment of malignant skeletal disease: initial experience with 18F-fluoride PET/CT and comparison between 18F-fluoride PET and 18Ffluoride PET/CT. J Nucl Med 2004;45:272–8. [PubMed: 14960647]
24. Meyers PA, Schwartz CL, Krailo M, et al. Osteosarcoma: a randomized, prospective trial of the addition of ifosfamide and/or muramyl tripeptide to cisplatin, doxorubicin, and high-dose methotrexate. J Clin Oncol 2005;23(9):2004–11. [PubMed: 15774791]
25. Cheon GJ, Kim MS, Lee JA, et al. Prediction model of chemotherapy response in osteosarcoma by 18F-FDG PET and MRI. J Nucl Med 2009;50: 1435–40. [PubMed: 19690035]
26. Ye Z, Zhu J, Tian M, et al. Response of osteogenic sarcoma to neoadjuvant therapy: evaluated by 18FFDG- PET. Ann Nucl Med 2008;22:475–80. [PubMed: 18670853]
27. Davis JC, Daw NC, Navid F, et al. ^{18}F-FDG uptake during early adjuvant chemotherapy predicts histologic response in pediatric and young adult patients with osteosarcoma. J Nucl Med 2018;59(1):25–30. [PubMed: 28611244]
28. Brenner W, Bohuslavizki KH, Eary JF. PET imaging of osteosarcoma. J Nucl Med 2003;44:930–42. [PubMed: 12791822]

29. Charest M, Hickeson M, Lisbona R, et al. FDG PET/CT imaging in primary osseous and soft tissue sarcomas: a retrospective review of 212 cases. Eur J Nucl Med Mol Imaging 2009;36(12):1944–51. [PubMed: 19593561]
30. Fuglø HM, Jørgensen SM, Loft A, et al. The diagnostic and prognostic value of 18F-FDG PET/CT in the initial assessment of high-grade bone and soft tissue sarcoma. A retrospective study of 89 patients. Eur J Nucl Med Mol Imaging 2012;39(9):1416–24. [PubMed: 22699526]
31. Hongtao L, Hui Z, Bingshun W, et al. 18F-FDG positron emission tomography for the assessment of histological response to neoadjuvant chemotherapy in osteosarcomas: a meta-analysis. Surg Oncol 2012; 21(4):e165–70. [PubMed: 22884956]
32. Franzius C, Daldrup-Link HE, Wagner-Bohn A, et al. FDG-PET for detection of recurrences from malignant primary bone tumors: comparison with conventional imaging. Ann Oncol 2002;13:157–60. [PubMed: 11863097]
33. Rakheja R, Makis W, Skamene S, et al. Correlating metabolic activity on 18F-FDG PET/CT with histopathologic characteristics of osseous and soft-tissue sarcomas: a retrospective review of 136 patients. AJR Am J Roentgenol 2012;198(6):1409–16. [PubMed: 22623556]
34. Buchbender C, Heusner TA, Lauenstein TC, et al. Oncologic PET/MRI, part 2: bone tumors, soft-tissue tumors, melanoma, and lymphoma. J Nucl Med 2012;53:1244–52. [PubMed: 22782313]
35. Purz S, Sabri O, Viehweger A. Potential pediatric applications of PET/MR. J Nucl Med 2014; 55(Supplement 2):32S–9S. [PubMed: 24762622]
36. Eiber M, Takei T, Souvatzoglou M, et al. Performance of whole-body integrated 18F-FDG PET/MR in comparison to PET/CT for evaluation of malignant bone lesions. J Nucl Med 2014;55:191–7. [PubMed: 24309383]
37. Denecke T, Hundsdörfer P, Misch D, et al. Assessment of histological response of paediatric bone sarcomas using FDG PET in comparison to morphological volume measurement and standardized MRI parameters. Eur J Nucl Med Mol Imaging 2010;37:1842–53. [PubMed: 20505933]
38. Ludwig JA. Ewing sarcoma: historical perspectives, current state of the art, and opportunities for targeted therapy in the future. Curr Opin Oncol 2008; 20:412–8. [PubMed: 18525337]
39. Kleis M, Daldrup-link H, Matthay K, et al. Diagnostic value of PET-CT for the staging and restaging of pediatric tumors. Eur J Nucl Med Mol Imaging 2009;36: 23–36. [PubMed: 18719909]
40. Guimarães JB, Rigo L, Lewin F, et al. The importance of PET/CT in the evaluation of patients with Ewing tumors. Radiol Bras 2015;48(3):175–80. [PubMed: 26185344]
41. London K, Stege C, Cross S, et al. 18F-FDG PET/CT compared to conventional imaging modalities in pediatric primary bone tumors. Pediatr Radiol 2012;42: 418–30. [PubMed: 22134535]
42. Bestic JM, Peterson JJ, Bancroft LW. Pediatric FDG PET/CT: physiologic uptake, normal variants, and benign conditions. Radiographics 2009;29(5): 1487–500. [PubMed: 19755607]
43. Arush MW, Israel O, Postovsky S, et al. Positron emission tomography/computed tomography with 18-fluorodeoxyglucose in the detection of local recurrence and distant metastases of pediatric sarcoma. Pediatr Blood Cancer 2007;49:901–5. [PubMed: 17252575]
44. Bredella MA, Caputo GR, Steinbach LS. Value of FDG positron emission tomography in conjunction with MR imaging for evaluating therapy response in patients with musculoskeletal sarcomas. AJR Am J Roentgenol 2002;179:1145–50. [PubMed: 12388489]
45. Hawkins DS, Schuetze SM, Butrynski JE, et al. [18F] Fluorodeoxyglucose positron emission tomography predicts outcome for Ewing sarcoma family of tumors. J Clin Oncol 2005;23:8828–34. [PubMed: 16314643]
46. Feldman F, Van Heertum R, Saxena C, et al. 18FDG-PET applications for cartilage neoplasms. Skeletal Radiol 2005;34(7):367–74. [PubMed: 15937711]
47. Jesus-Garcia R, Osawa A, Filippi RZ, et al. Is PET-CT an accurate method for the differential diagnosis between chondroma and chondrosarcoma? Springer-plus 2016;5:236. [PubMed: 27026930]
48. Brenner W, Conrad EU, Eary JF. FDG PET imaging for grading and prediction of outcome in chondrosarcoma patients. Eur J Nucl Med Mol Imaging 2004;31:189–95. [PubMed: 15129700]

49. Subhawong TK, Winn A, Shemesh SS. F-18 FDG PET differentiation of benign from malignant chondroid neoplasms: a systematic review of the literature. Skeletal Radiol 2017;46(9):1233–9. [PubMed: 28608242]
50. Lee FY-I, Yu J, Chang S-S, et al. Diagnostic value and limitations of fluorine-18 fluorodeoxyglucose positron emission tomography for cartilaginous tumors of bone. J Bone Joint Surg am 2004;86–A(12):2677–85.
51. Costelloe CM, Chuang HH, Chasen BA, et al. Bone windows for distinguishing malignant from benign primary bone tumors on FDG PET/CT. J Cancer 2013;4(7):524–30. [PubMed: 23983816]
52. Sheikhbahaei S, Marcus C, Hafezi-Nejad N, et al. Value of FDG PET/CT in patient management and outcome of skeletal and soft tissue sarcomas. PET Clin 2015;10(3):375–93. [PubMed: 26099673]
53. Purohit BS, Dulguerov P, Burkhardt K, et al. Dedifferentiated laryngeal chondrosarcoma: combined morphologic and functional imaging with positron-emission tomography/magnetic resonance imaging. Laryngoscope 2014;124(7):E274–7. [PubMed: 24222068]
54. Singh T, Satheesh CT, Lakshmaiah KC, et al. Primary bone lymphoma: a report of two cases and review of the literature. J Cancer Res Ther 2010;6(3): 296–8. [PubMed: 21119256]
55. Kitsoulis P, Vlychou M, Papoudou-Bai A, et al. Primary lymphomas of bone. Anticancer Res 2006; 26(1A):325–37. [PubMed: 16475714]
56. Bosch-Barrera J, Arbea L, García-Velloso MJ, et al. Primary bone lymphoma of mandible and thyroid incidentaloma identified by FDG PET/CT: a case report. Cases J 2009;2:6384. [PubMed: 19829800]
57. Kwee TC, Kwee RM, Nievelstein RA. Imaging in staging of malignant lymphoma: a systematic review. Blood 2008;111:504–16. [PubMed: 17916746]
58. Hutchings M, Barrington SF. PET/CT for therapy response assessment in lymphoma. J Nucl Med 2009;50(Suppl 1):21S–30S. [PubMed: 19380407]
59. Catlett JP, Williams SA, O'Connor SC, et al. Primary lymphoma of bone: an institutional experience. Leuk Lymphoma 2008;49:2125–32. [PubMed: 19021055]
60. Breiback F, Julian A, Laurent C, et al. Contribution of the 2-[18F]- fluoro-s-deoxy-D-glucose positron emission tomography/computed tomography to the diagnosis of primary osseous Hodgkin lymphoma. BMJ Case Rep 2009;2009 Available at: http://www.ncbi.nlm.nih.gov/pubmed/21686679. Accessed January 14, 2014.
61. Lin EC. FDG PET/CT flip flop phenomenon in treated lymphoma of bone. Clin Nucl Med 2006; 31(12):803–5. [PubMed: 17117078]
62. Park YH, Kim S, Choi SJ, et al. Clinical impact of whole-body FDGPET for evaluation of response and therapeutic decision-making of primary lymphoma of bone. Ann Oncol 2005;16(8): 1401–2. [PubMed: 15870088]
63. Huan Y, Qi Y, Zhang W, et al. Primary bone lymphoma of radius and tibia: a case report and review of literature. Medicine (Baltimore) 2017;96(15):e6603. [PubMed: 28403103]
64. Rakheja R, Chandarana H, DeMello L, et al. Correlation between standardized uptake value and apparent diffusion coefficient of neoplastic lesions evaluated with whole-body simultaneous hybrid PET/MRI. AJR Am J Roentgenol 2013;201:1115–9. [PubMed: 24147485]
65. Wu X, Korkola P, Pertovaara H, et al. No correlation between glucose metabolism and apparent diffusion coefficient in diffuse large B-cell lymphoma: a PET/CT and DW-MRI study. Eur J Radiol 2011;79: e117–21. [PubMed: 21596501]
66. Hagtvedt T, Seierstad T, Lund KV, et al. Diffusion weighted MRI compared to FDG PET/CT for assessment of early treatment response in lymphoma. Acta Radiol 2015;56(2):152–8. [PubMed: 24585944]
67. International Myeloma Working Group. Criteria for the classification of monoclonal gammopathies, multiple myeloma and related disorders: a report of the International Myeloma Working Group. Br J Haematol 2003;121(5):749–57. [PubMed: 12780789]
68. Dimopoulos M, Terpos E, Comenzo RL, et al. International Myeloma Working Group consensus statement and guidelines regarding the current role of imaging techniques in the diagnosis and monitoring of multiple myeloma. Leukemia 2009;23: 1545–56. [PubMed: 19421229]

69. Bartel TB, Haessler J, Brown TL, et al. F18-fluorodeoxyglucose positron emission tomography in the context of other imaging techniques and prognostic factors in multiple myeloma. Blood 2009;114(10): 2068–76. [PubMed: 19443657]
70. Dammacco F, Rubini G, Ferrari C, et al. (18)F-FDG PET/CT: a review of diagnostic and prognostic features in multiple myeloma and related disorders. Clin Exp Med 2006;15(1):1–8.
71. Fechtner K, Hillengass J, Delorme S, et al. Staging monoclonal plasma cell disease: comparison of the Durie-Salmon and the Durie-Salmon plus staging systems. Radiology 2010;257(1):195–204. [PubMed: 20851941]
72. Breyer RJ, Mulligan ME, Smith SE, et al. Comparison of imaging with FDG PET/CT with other imaging modalities in myeloma. Skeletal Radiol 2006;35: 632–40. [PubMed: 16758246]
73. Schirrmeister H, Bommer M, Buck AK, et al. Initial results in the assessment of multiple myeloma using 18F-FDG PET. Eur J Nucl Med Mol Imaging 2002; 29:361–6. [PubMed: 12002711]
74. Zamagni E, Nanni C, Gay F, et al. 18F-FDG PET/CT focal, but not osteolytic, lesions predict the progression of smoldering myeloma to active disease. Leukemia 2016;30(2):417–22. [PubMed: 26490489]
75. Shortt CP, Gleeson TG, Breen KA, et al. Whole-Body MRI versus PET in assessment of multiple myeloma disease activity. AJR Am J Roentgenol 2009;192: 980–6. [PubMed: 19304704]
76. Shah SN, Oldan JD. PET/MR imaging of multiple myeloma. Magn Reson Imaging Clin N Am 2017; 25(2):351–65. [PubMed: 28390534]
77. Purohit S, Pardiwala D. Imaging of giant cell tumor of bone. Indian J Orthop 2007;41(2):91–6. [PubMed: 21139758]
78. Gong L, Liu W, Sun X, et al. Histological and clinical characteristics of malignant giant cell tumor of bone. Virchows Arch 2012;460:327–34. [PubMed: 22350004]
79. Feigenberg SJ, Marcus RB Jr, Zlotecki RA, et al. Whole-lung radiotherapy for giant cell tumors of bone with pulmonary metastases. Clin Orthop Relat Res 2002;(401):202–8.
80. Park HL, Yoo IR, Lee Y, et al. Giant Cell tumor of the rib: two cases of F-18 FDG PET/CT findings. Nucl Med Mol Imaging 2017;51(2):182–5. [PubMed: 28559944]
81. Hoshi M, Takada J, Oebisu N, et al. Overexpression of hexokinase-2 in giant cell tumor of bone is associated with false positive in bone tumor on FDG-PET/CT. Arch Orthop Trauma Surg 2012;132: 1561–8. [PubMed: 22825642]
82. Muheremu A, Ma Y, Huang Z, et al. Diagnosing giant cell tumor of the bone using positron emission tomography/computed tomography: a retrospective study of 20 patients from a single center. Oncol Lett 2017;14(2):1985–8. [PubMed: 28781642]
83. Makis W, Alabed YZ, Nahal A, et al. Giant cell tumor pulmonary 18 metastases mimic primary malignant pulmonary nodules on FFDGPET/CT. Nucl Med Mol Imaging 2012;46:134–7. [PubMed: 24900048]
84. Gholamrezanezhad A, Chirindel A, Subramaniam R. Assessment of response to therapy In: Peller P, Subramaniam R, Guermazi A, editors. PET-CT and PET-MRI in oncology. Medical radiology. Berlin (Germany): Springer; 2012 p. 279–322.
85. Boye K, Jebsen NL, Zaikova O, et al. Denosumab in patients with giant-cell tumor of bone in Norway: results from a nationwide cohort. Acta Oncol 2017; 56(3):479–83. [PubMed: 28105885]
86. Gholamrezanezhad A, Basques K, Batouli A, et al. Applications of PET/CT and PET/MRI in Musculoskeletal, Orthopedic, and Rheumatologic Imaging. AJR Am J Roentgenol 2018;210(6):245–63.
87. Gholamrezanezhad A, Mehrkhani F, Olyaie M. Imaging approach in the evaluation of response to treatment of breast cancer. Nucl Med Commun 2018; 39(4):343–4. [PubMed: 29533346]

KEY POINTS

- The hybrid modalities of FDG PET/CT and PET/MRI have improved oncologic imaging that combine the sensitivity of metabolic imaging with the specificity of anatomic imaging.
- PET/CT is a valuable modality in the diagnosis, staging, and assessment of therapeutic response to treatment of several primary musculoskeletal malignancies.
- PET/MRI is promising modality, which allowed detailed local staging and tissue characterization, all while reducing patient's exposure to radiation.

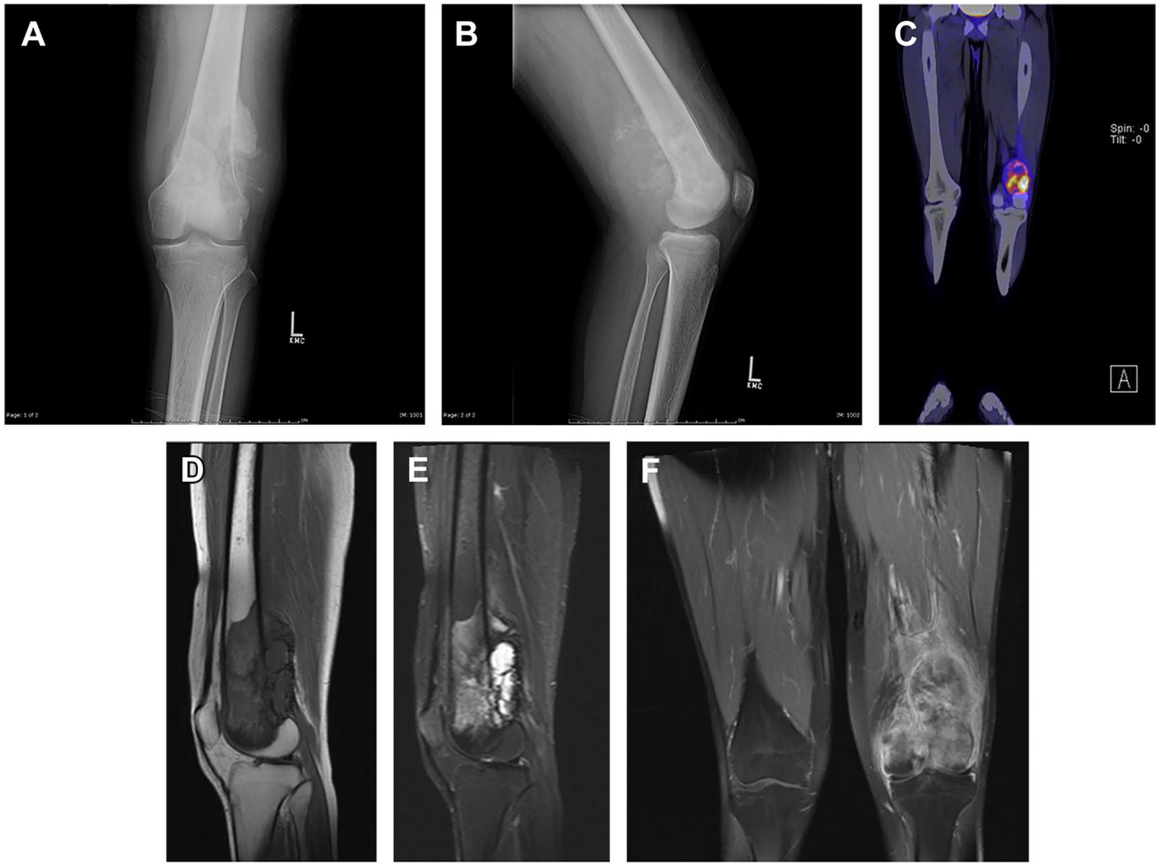

Fig. 1.

A 19-year-old man presented with left knee pain for 1 month. The radiograph (*A*, *B*) shows aggressive osteolytic lesion of the distal left femur with sunburst periosteal reaction. The lesion demonstrates heterogeneous increased metabolic activity on PET/CT with fludeoxyglucose F 18 (FDG) with a maximum standardized uptake value of 8.8 (*C*). On MRI, the lesion demonstrates heterogeneous intermediate signal intensity on T1-weighted imaging (*D*), hypersignal on short tau inversion recovery imaging (*E*), and heterogeneous postcontrast enhancement (*F*) with cortical breakthrough, aggressive periosteal reaction, and associated soft tissue mass. Histopathologic evaluation confirmed osteosarcoma.

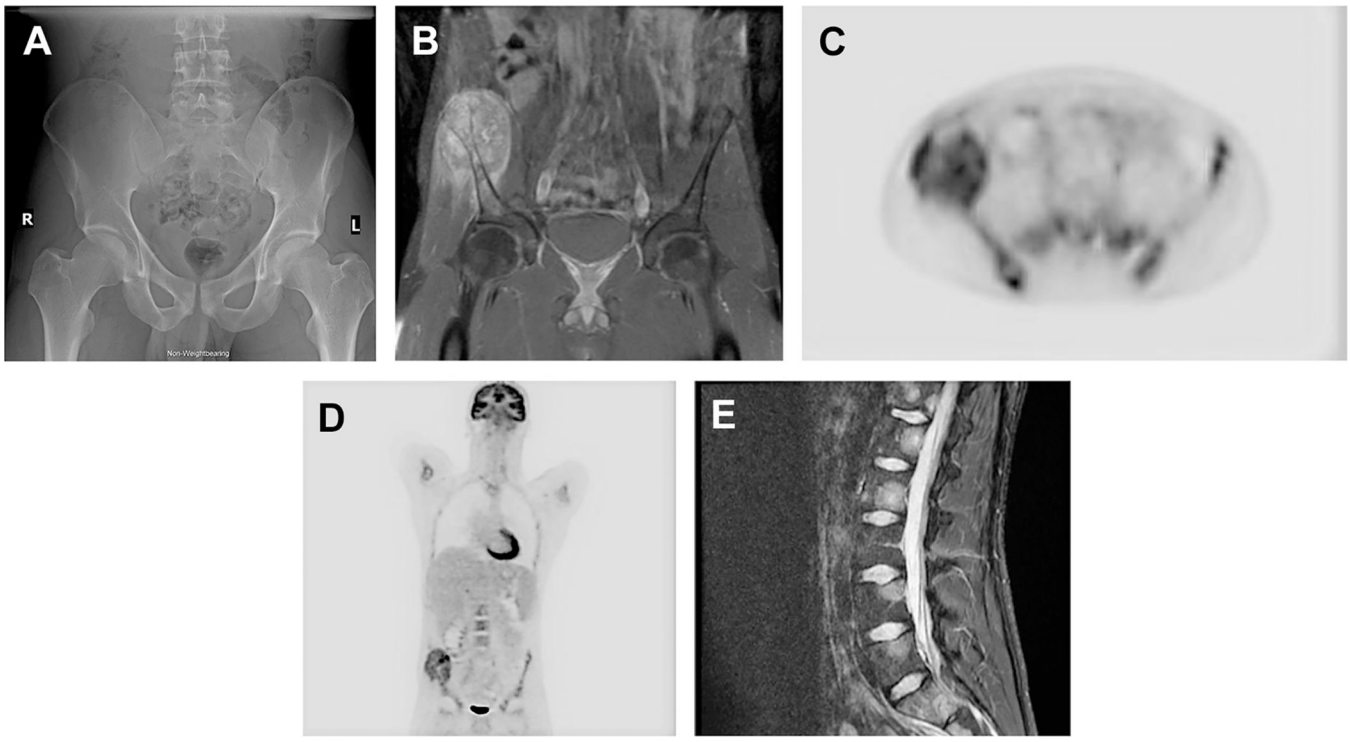

Fig. 2.

A 21-year-old man presented with right hemipelvic pain. Initial radiographs were interpreted as unremarkable, but retrospectively demonstrated asymmetric thinning of the right iliac and suspect rarefaction of the right iliac bone compared with the contralateral side (*A*). On MRI (*B*), a large enhancing destructive lesion involving the anterior right iliac crest was identified, the biopsy of which showed Ewing's sarcoma. PET/CT with fludeoxyglucose F 18 for initial staging demonstrated a heterogeneously hypermetabolic lesion centered at the right iliac crest with maximum standardized uptake value of 8.2 and several metastatic foci involving the posterior right iliac crest, left hemisacrum, and thoracolumbar spine (*C*, *D*). MRI of the spine confirmed metastatic disease to the vertebrae (*E*).

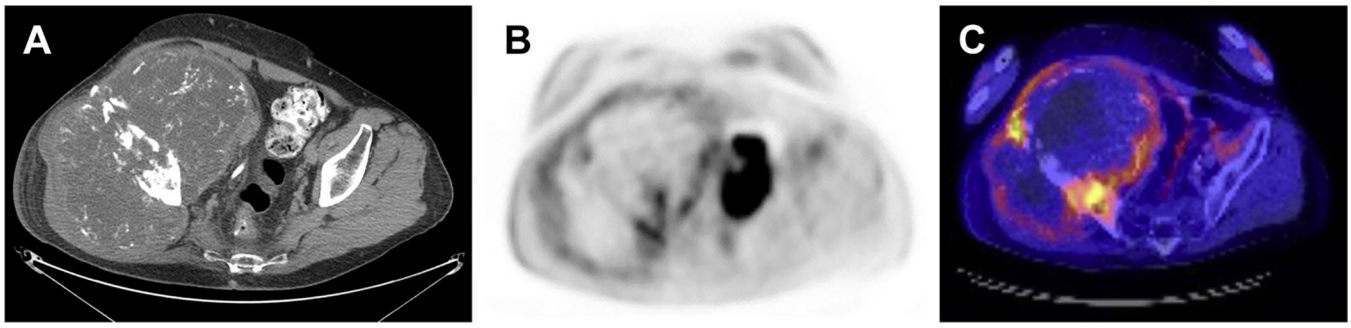

Fig. 3.

A 72-year-old man with history of pathologically proven chondrosarcoma presented with recurrent mass at the right iliac fossa. Computed tomography scanning demonstrated a large heterogeneous mass with chondroid matrix, concerning for recurrent chondrosarcoma (*A*). On PET with fludeoxyglucose F 18, a 19.4 × 13.3 × 17.6 cm heterogeneous destructive mass centered at the right iliac bone was identified, demonstrating peripheral hypermetabolism and central hypometabolism, representing large central necrosis. The maximum standardized uptake value was 9.4 (*B*, *C*).

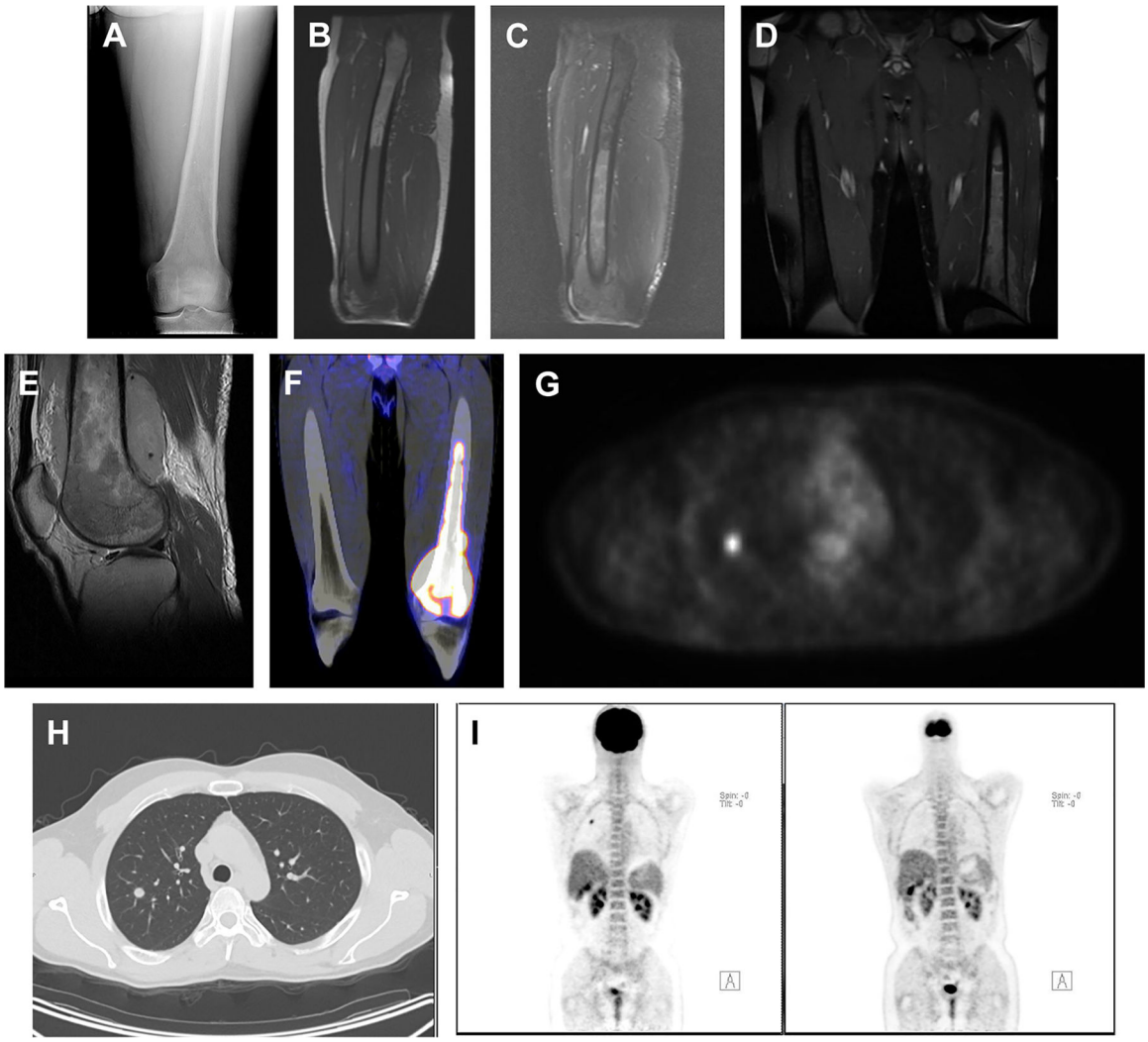

Fig. 4.

A 40-year-old man with left knee pain demonstrated a permeative osteolytic lesion of the distal left femur (*A*). On MRI, a large marrow-replacing lesion was identified, which shows decreased T1-weighted uptake (*B*) and heterogeneously increased short tau inversion recovery (*C*) hypersignal intensity with heterogeneous postcontrast enhancement (*D*, *E*). The lesion is intensely hypermetabolic on PET with maximum standardized uptake value of 17.3 (*F*). The lesion was pathologically diagnosed as T-cell lymphoma. There is a small, metabolically active soft tissue density pulmonary nodule within the right lobe with maximum standardized uptake value of 3.7 (*G*, *H*), concerning for a metastatic lesion. The pulmonary lesion was completely resolved on postchemotherapy PET (*I*).

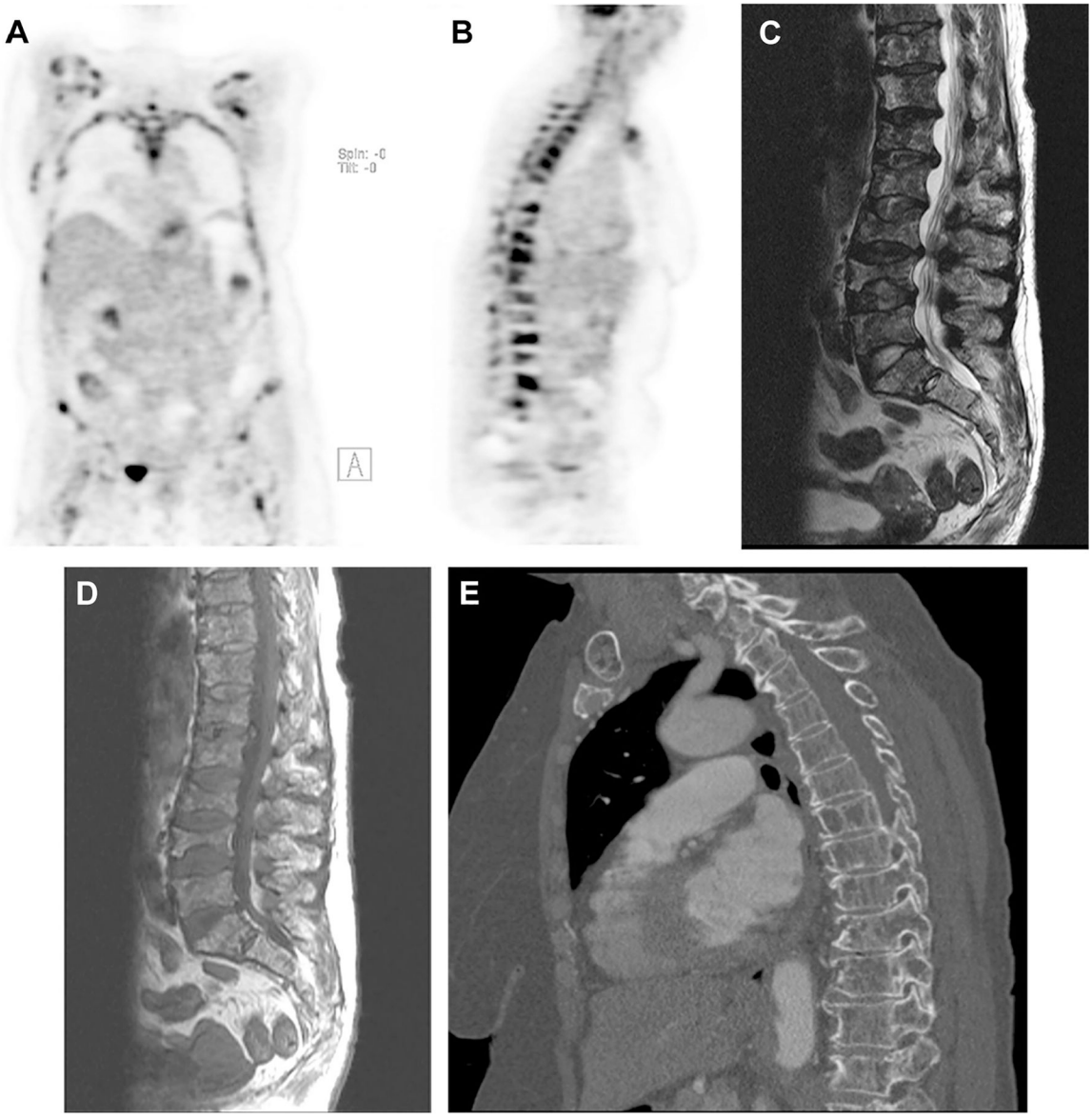

Fig. 5.

A 65-year-old woman with generalized bone pain and anemia was diagnosed with multiple myeloma. PET-computed tomography (CT) scans revealed widespread osseous (*A*) myelomatous lesions with several infiltrative lesions of the spine (*B*) and superimposed pathologic fractures, as confirmed on MRI (*C*, *D*) and CT (*E*). The maximum standardized uptake value of the lesions in the lumbar spine was up to 17.2.